doi:10.1093/brain/awz056 BRAIN 2019: 0; 1–13 | 1

BRAIN
A JOURNAL OF NEUROLOGY

Dissociating thalamic alterations in alcohol use disorder defines specificity of Korsakoff's syndrome

Shailendra Segobin,[1] Alice Laniepce,[1] Ludivine Ritz,[1] Coralie Lannuzel,[1] Céline Boudehent,[1,2] Nicolas Cabé,[1,2] Laurent Urso,[3] François Vabret,[1,2] Francis Eustache,[1] Hélène Beaunieux[1] and Anne-Lise Pitel[1]

The thalamus, a relay organ consisting of several nuclei, is shared between the frontocerebellar circuit and the Papez circuit, both particularly affected in alcohol use disorder. Shrinkage of the thalamus is known to be more severe in alcoholics with Korsakoff's syndrome than in those without neurological complications (uncomplicated alcoholics). While thalamic atrophy could thus be a key factor explaining amnesia in Korsakoff's syndrome, the loci and nature of alterations within the thalamic nuclei in uncomplicated alcoholics and alcoholics with Korsakoff's syndrome remains unclear. Indeed, the literature from animal and human models is disparate regarding whether the anterior thalamic nuclei, or the mediodorsal nuclei are particularly affected and would be responsible for amnesia. Sixty-two participants (20 healthy controls, 26 uncomplicated alcoholics and 16 patients with Korsakoff's syndrome) underwent a diffusion tensor imaging sequence and T_1-weighted MRI. State-of-the-art probabilistic tractography was used to segment the thalamus according to its connections to the prefrontal cortex and cerebellar Cruses I and II for the frontocerebellar circuit's executive loop, the precentral gyrus and cerebellar lobes IV–VI for the fronto-cerebellar circuit's motor loop, and hippocampus for the Papez circuit. The connectivity and volumes of these parcellations were calculated. Tractography showed that the hippocampus was principally connected to the anterior thalamic nuclei while the prefrontal cortex was principally connected to the mediodorsal nuclei. The fibre pathways connecting these brain regions and their respective thalamic nuclei have also been validated. ANCOVA, with age and gender as covariates, on connectivity measures showed abnormalities in both patient groups for thalamic parcellations connected to the hippocampus only [$F(2,57) = 12.1$; $P < 0.0001$; $\eta^2 = 0.2964$; with graded effects of the number of connections from controls to uncomplicated alcoholics to Korsakoff's syndrome]. Atrophy, on the other hand, was observed for the prefrontal parcellation in both patient groups and to the same extent compared to controls [$F(2,56) = 18.7$; $P < 0.0001$; $\eta^2 = 0.40$]. For the hippocampus parcellation, atrophy was found in the Korsakoff's syndrome group only [$F(2,56) = 5.5$; $P = 0.006$; $\eta^2 = 0.170$, corrected for multiple comparisons using Bonferroni, $P < 0.01$]. *Post hoc* Tukey's test for unequal sample sizes, healthy controls > patients with Korsakoff's syndrome ($P = 0.0036$). Two different mechanisms seem to affect the thalamus. In the frontocerebellar circuit, atrophy of the mediodorsal nuclei may lead to the alterations, whereas in the Papez circuit, disconnection between the anterior nuclei and hippocampus may be the leading factor. Shrinkage of the anterior nuclei could be specific to patients with Korsakoff's syndrome, hence a potential neuroimaging marker of its pathophysiology, or more generally of thalamic amnesia for which Korsakoff's syndrome has historically been used as a model.

1 Normandie Univ, UNICAEN, PSL Research University, EPHE, INSERM, U1077, CHU de Caen, Cyceron, Neuropsychologie et Imagerie de la Mémoire Humaine, 14000 Caen, France
2 Service d'Addictologie, Centre Hospitalier Universitaire de Caen, 14000 Caen, France
3 Service d'Addictologie, Centre Hospitalier Roubaix, 59056 Roubaix, France

Received October 23, 2018. Revised December 23, 2018. Accepted January 20, 2019

Correspondence to: Dr Shailendra Segobin
GIP Cyceron
Boulevard Henri Becquerel
F-14074 Caen Cedex
France
E-mail: segobin@cyceron.fr

Keywords: Korsakoff's syndrome; diffusion tensor imaging; segmentation; anterior thalamic nuclei; mediodorsal thalamic nuclei

Abbreviations: AUD = alcohol use disorder; DTI = diffusion tensor imaging; FCC = frontocerebellar circuit

Introduction

Korsakoff's syndrome is a severe neurological disorder stemming from a combination of chronic and excessive alcohol consumption and altered thiamine metabolism (Kopelman *et al.*, 2009). It mainly results in severe amnesia and is potentially associated with executive deficits and ataxia. 'Uncomplicated' alcoholics, i.e. patients with alcohol use disorder (AUD) without such ostensible and severe neurological complications, are heterogeneous as some have preserved cognitive performances while others can have deficits close to those of patients with Korsakoff's syndrome (Pitel *et al.*, 2008).

In both uncomplicated alcoholics and patients with Korsakoff's syndrome, two brain networks and associated cognitive functions are predominantly affected: the frontocerebellar circuit (FCC) and the Papez circuit (Papez, 1937; Chanraud *et al.*, 2010; Pitel *et al.*, 2014). Both functional circuits have been well described structurally in terms of grey matter nodes (Papez, 1937; Kelly and Strick, 2003) and the potential white matter tracts that connect them (Mori *et al.*, 2010; Segobin *et al.*, 2015). The FCC consists of two parallel closed loops, one executive [Brodmann areas (BA) 9 and 46; pons; cerebellar cruses I and II] and one motor (cerebellar lobes IV–VI; pons and motor cortex). The Papez circuit encompasses the hippocampus, mammillary bodies and cingulate gyrus. The thalamus is shared between the FCC and Papez circuit and has been described as 'the gateway to the cortex' (Sherman and Guillery, 2001).

The effect of AUD on the thalamus has been documented mostly through the prism of Korsakoff's syndrome via neuropathological and neuroimaging studies. In fact, patients with Korsakoff's syndrome have historically been used as a model for understanding the pathophysiological mechanisms underpinning thalamic/diencephalic amnesia (Kopelman, 2015). Generally, the thalamus was found to be affected in both uncomplicated alcoholics and those with Korsakoff's syndrome (Harding *et al.*, 2000; Kopelman *et al.*, 2009; Pitel *et al.*, 2014). Furthermore, graded effects were found in grey matter thalamic shrinkage from uncomplicated alcoholics to patients with Korsakoff's syndrome (Sullivan and Pfefferbaum, 2008; Pitel *et al.*, 2012). Histological examinations have pointed towards the mediodorsal nuclei and the anterior nuclei of the thalamus as being especially affected in AUD (Victor *et al.*, 1971; Harding *et al.*, 2000). However, the specificity of these two nuclei, in terms of how they contribute towards the FCC or the Papez circuit, and how they are differentially altered in uncomplicated alcoholics and Korsakoff's syndrome patients, is still under debate (Aggleton, 2012; Carlesimo *et al.*, 2014; Pitel *et al.*, 2014; Kopelman, 2015). While several studies involving both human and animal models have suggested that the mediodorsal nuclei could be critically affected in Korsakoff's syndrome (Victor *et al.*, 1971; Pitel *et al.*, 2012; Savage *et al.*, 2012), hence explaining their anterograde amnesia, others have pointed towards lesions in the anterior nuclei as being key to this pathology (Mair *et al.*, 1979; Mayes *et al.*, 1988; Harding *et al.*, 2000).

Neuroimaging in humans has provided little to no evidence regarding the loci and nature of thalamic lesions at nuclear level. Conventional structural MRI sequences in the whole brain do not provide for high resolution contrast between the different thalamic nuclei. However, development of diffusion tensor imaging (DTI) sequences, in tandem with state-of-the-art probabilistic tractography algorithms now allows the estimation of the number of white matter fibres connecting two regions at a voxel level (Behrens *et al.*, 2003, 2007; Johansen-Berg *et al.*, 2005). It is therefore possible to segment the thalamus into parcellations that connect to key nodes of the FCC and Papez circuit, defined *a priori*, and estimate the number of fibre tracts contained in each parcellation. Corresponding volumes of these parcellations can subsequently be obtained through high resolution T_1-weighted MRI. Using these refined measurements, our objectives were (i) to identify which intra-thalamic regions the nodes of the FCC and Papez circuit were connected to; and (ii) to specify the mechanisms (specific thalamic shrinkage and/or disconnection) that lead to the brain pathophysiology in uncomplicated alcoholics and patients with Korsakoff's syndrome for each brain circuit.

Materials and methods

Population

Forty-two patients (28 males, 14 females) with AUD (DSM-5 criteria, American Psychiatric Association, 2013) and 20 healthy subjects (15 males, five females) were included in the study.

Of the 42 AUD patients, 16 (seven males, nine females) filled the DSM-5 criteria for alcohol-induced major neurocognitive disorder, amnestic-confabulatory type, persistent and were therefore diagnosed as patients with Korsakoff's syndrome. They were recruited as inpatients at Caen University Hospital ($n = 8$) and in a nursing home (Maison Vauban, Roubaix, France; $n = 8$). All patients with Korsakoff's syndrome had a history of heavy drinking (longer than 20 years), but it was difficult to obtain accurate information about their alcohol intake because of their amnesia. The background information for the patients with Korsakoff's syndrome came mainly from family members and medical records. For each patient with Korsakoff's syndrome, the selection was made according to a codified procedure in a French officially registered centre for addiction. The case of each patient was examined by a multidisciplinary team made up of specialists in cognitive neuropsychology and behavioural neurology. A detailed neuropsychological examination enabled the diagnosis of all Korsakoff's syndrome patients presenting disproportionately severe episodic memory disorders compared to other cognitive functions (Table 1). The consequences of their memory impairments were such that none of the patients with Korsakoff's syndrome were able to return to their previous jobs and all lived in sheltered accommodation or were inpatients waiting for a place in an institution. Clinical and neuroimaging investigations ruled out other possible causes of memory impairments (particularly focal brain damage).

The 26 AUD patients without Korsakoff's syndrome were considered as 'uncomplicated alcoholic patients'. They were recruited by clinicians while being inpatients for AUD at Caen University Hospital. Although patients were in early abstinence (16.7 ± 21.4 days of sobriety prior to inclusion), none of them presented with physical symptoms of alcohol withdrawal as assessed by the Cushman's scale (Cushman *et al.*, 1985) at inclusion. They were interviewed with the Alcohol Use Disorders Identification Test (AUDIT) (Gache *et al.*, 2005) and a modified version of the semi-structured lifetime drinking history (Pfefferbaum *et al.*, 1988). Measures included the duration of alcohol use (in years), alcohol misuse (in years), number of withdrawal and daily alcohol consumption prior to treatment (in units, a standard drink corresponding to a beverage containing 10 g of pure ethanol).

The control group (healthy controls) was recruited locally and matched the demographics of the uncomplicated alcoholics. Inclusion criteria were: a minimum Mini-Mental State Examination (MMSE) score of 26 or a minimum Mattis Dementia Rating score of 129, and a maximum Beck Depression Inventory (BDI) of 29. The maximum AUDIT score was 6 for females and 7 for males.

To be included, all participants had to be between 18 and 70 years old, and to have French as their native language. No participant had a co-morbid psychiatric disorder, taking psychotropic medication, had a history of serious chronic pathology (diabetes, hepatitis, HIV, endocrinal disorder, as revealed by participants' blood tests), neurological problems (traumatic head injury causing loss of consciousness for > 30 min, epilepsy, stroke, etc.) that might have affected cognitive function. No participant fulfilled the DSM-5 criteria for use disorder of another substance over the last 3 months (except tobacco). They had not taken any other psychoactive substance more than five times over the last month (except alcohol for the patients). All participants were also evaluated for any signs of lacunar stroke, small vessel diseases or any overt vascular damage. We systematically performed this evaluation through a FLAIR sequence and a T_2* sequence. The images were scrutinized by a neurologist who validated the inclusion of the patient in our research protocol, having excluded patients that potentially showed any form of neurological alterations due to any pathology other than that linked with the pathophysiology of AUD. All participants gave their informed written consent to the study, which was approved by the local ethics committee. The study was carried out in line with the Declaration of Helsinki (1964).

Uncomplicated alcoholics and healthy controls were age- and education-matched ($P = 0.72$ and $P = 0.76$, respectively). Patients with Korsakoff's syndrome differed from both healthy controls and uncomplicated alcoholics in age, education (years of schooling) and MMSE scores. Age, education, depression (BDI), and anxiety scores (State-Trait Anxiety Inventory, STAI) (Spielberger *et al.*, 1983) as well as nicotine dependence level are reported in Table 1.

Acquisition of neuroimaging data

Volumetric data

A high-resolution T_1-weighted anatomical image was acquired for each subject on a Philips Achieva 3 T scanner using a 3D fast-field echo sequence (sagittal; repetition time = 20 ms; echo time = 4.6 ms; flip angle = 10°; 180 slices; slice thickness, 1 mm; field of view, 256×256 mm^2; matrix, 256×256).

DTI data

All participants also underwent a DTI sequence on the same scanner. Seventy slices (slice thickness of 2 mm, no gap) were acquired axially using a DTI spin echo (DWI-SE) sequence (32 directions at b = 1000 s/mm^2, repetition time = 10 000 ms; echo time = 82 ms; flip angle = 90°, field of view = 224×224 mm^2; matrix = 112×112 and in-plane resolution of 2×2 mm^2). One no-diffusion weighted image at b = 0 s/mm^2 was also acquired.

Processing of neuroimaging data

Volumetric data processing

Volumetric datasets were preprocessed using the SPM12 toolbox (https://www.fil.ion.ucl.ac.uk/spm/software/spm12/ Statistical Parametric Mapping software; Wellcome Department of Cognitive Neurology, Institute of Neurology, London, UK). T_1-weighted images were segmented into grey matter and spatially normalized to the Montreal Neurological Institute (MNI) space (voxel size = 1.5 mm^3; matrix = $121 \times 145 \times 121$). The normalized grey matter images were modulated by the Jacobian determinants to preserve volume concentrations. The normalization parameters (forward and inverse) were also saved to generate the required thalamic seed and regional target masks for the thalamus classification step, and for the subsequent calculation of thalamic parcellated volumes. The flowchart describing the image processing steps is shown in Fig. 1.

Table 1 Demographic, clinical and neuropsychological description of the control participants and alcoholics with and without Korsakoff's syndrome

Variable	HC (*n* = 20) M = 15; F = 5	UA (*n* = 26) M = 21; F = 5	KS (*n* = 6) M = 7; F = 9	Group differences[a]
Demographic data				
Age[b], years	44.5 ± 6.8 [31–55]	46.6 ± 8.5 [33–66]	55.9 ± 5.7 [44–67]	HC = UA HC < KS (P = 0.0002) UA < KS (P = 0.0016)
Education, years	11.5 ± 2.1 [9–15]	11.9 ± 1.9 [9–15]	9.9 ± 2.1 [6–15]	HC = UA = KS
AUDIT	2.8 ± 1.5 [0–5]	29.4 ± 6.9 [9–39]	15.0 ± 13.6 [1–37]	HC < UA (P = 0.0001) HC < KS (P = 0.0034) KS < UA (P = 0.0006)
BDI	3.8 ± 3.7 [0–14]	11.3 ± 7.4 [2–27]	7.9 ± 8.0 [0–29]	HC < UA (P = 0.0021) HC = KS UA = KS
STAI[c] A	27.3 ± 7.0 [20–47]	29.9 ± 10.4 [20–59]	30.5 ± 9.5 [20–51]	HC = UA = KS
STAI[c] B	33.6 ± 7.1 [23–50]	43.0 ± 11.9 [28–66]	38.7 ± 11.3 [24–57]	HC < UA (P = 0.0152) HC = KS UA = KS
Fagerstrom[d]	0.6 ± 1.5 [0–6]	4.4 ± 3.5 [0–14]	4.0 ± 4.0 [0–10]	HC < UA (P = 0.0002) HC = KS UA = KS
Clinical data				
Abstinence before inclusion, days	N/A	11.4 ± 5.0 [4–24]	N/A	
Alcohol use, years	N/A	31.3 ± 9.4 [18–51]	N/A	
Alcohol misuse, years	N/A	19.7 ± 9.1 [2–34]	N/A	
Alcohol dependence, years	N/A	9.9 ± 8.1 [1–34]	N/A	
Alcohol consumption over last 30 days	N/A	20.0 ± 9.0 [0–40]	N/A	
Number of previous detoxifications	N/A	2.5 ± 2.4 [0–11]	N/A	
Neuropsychological data				
Global cognitive evaluation				
MMSE (/30)	28.6 ± 1.1 [27–30]	27.1 ± 2.7 [20–30]	23.6 ± 2.6 [18–27]	HC > KS (P = 0.0001) UA > KS (P = 0.0003)
Mattis total score	141 ± 2.0 [136–144]	135 ± 8.5 [107–143]	120 ± 9.9 [95–133]	HC > UA (P = 0.0254) HC > KS (P = 0.0001) UA > KS (P = 0.0001)
Verbal episodic memory				
FSCRT: sum of three free recalls	33.6 ± 4.9	28.1 ± 8.6	5.9 ± 2.9	HC > UA (P = 0.0403) HC > KS (P = 0.0001) UA > KS (P = 0.0001)
CVLT: sum of five immediate recalls	62.2 ± 6.6	53.8 ± 17.2	23.4 ± 11.0	HC = UA (P = 0.0877) HC > KS (P = 0.0001) UA > KS (P = 0.0001)
Executive functions				
MCST: number of perseverative responses	0.95 ± 1.2	2.8 ± 3.4	5.4 ± 4.7	HC = UA HC < KS (P = 0.0079) UA = KS

Mean ± standard deviation and range [minimum–maximum] are reported. *Post hoc* HSD Tukey for unequal sample sizes (P-values shown for when $P < 0.05$).

[a]ANCOVA with age and gender as covariate $F(2,57)$.

[b]ANCOVA with gender as covariate $F(2,58)$.

[c]State-Trait Anxiety Inventory (STAI) for adults, Y-A for 'state anxiety' and Y-B for 'trait anxiety'.

[d]Fagerstrom.

Note: Alcohol drinking history data for patients with Korsakoff's syndrome could either not be obtained or their accuracy could not be verified.

AUDIT = Alcohol Use Disorders Test; BDI = Beck Depression Inventory; CVLT = California Verbal Learning Test; F = female; FSCRT = Free and Cued Selective Reminding Test; HC = healthy controls; KS = alcoholics with Korsakoff's syndrome; M = male; MCST = Modified Card Sorting Test; MMSE = Mini-Mental State Examination; N/A = not available; UA = uncomplicated alcoholics.

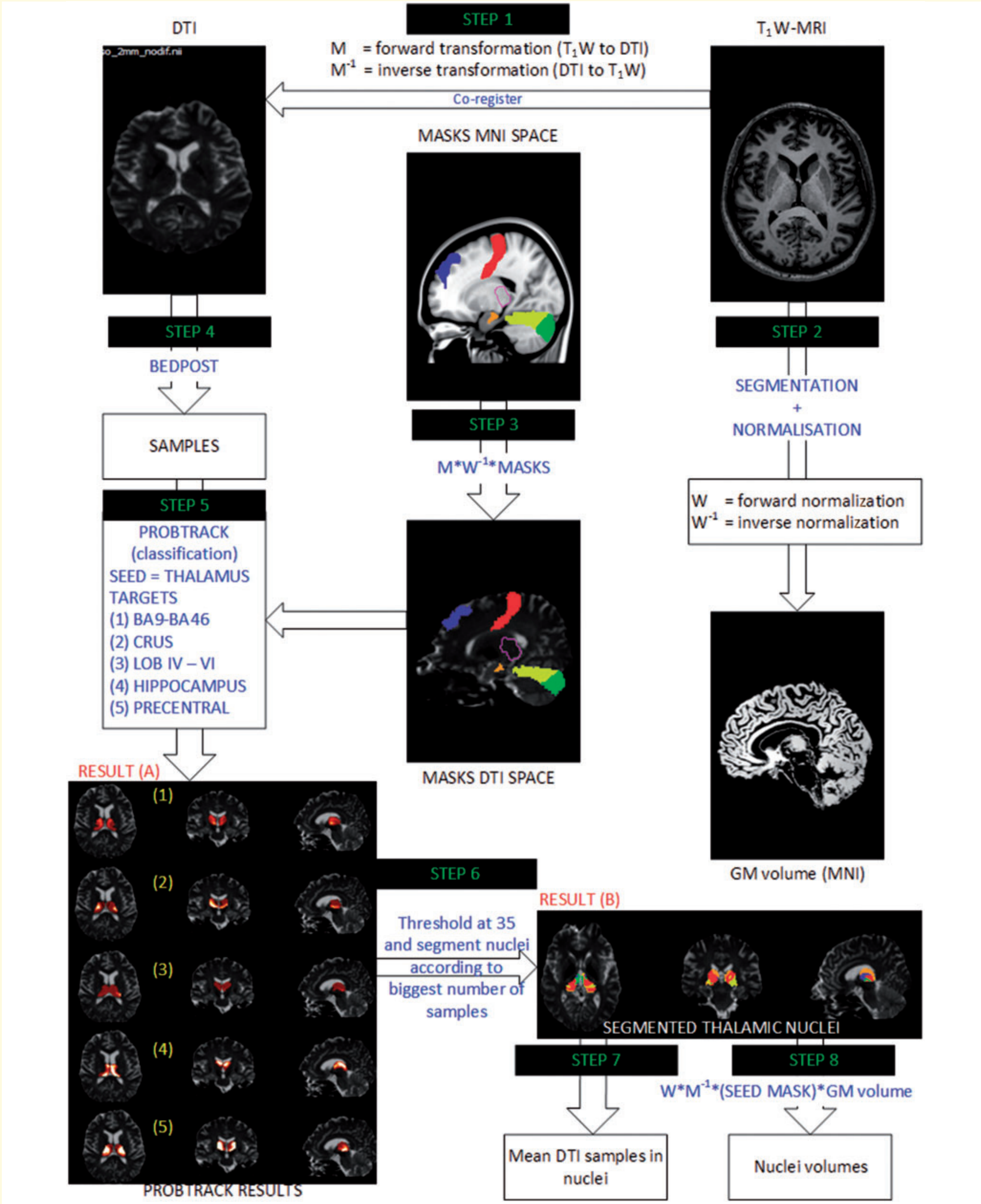

Figure 1 Processing steps for the anatomical T_1-weighted image and the DTI sequence to output mean number of connections per sub-nuclei and their corresponding volumes. Step 1: The T_1-weighted-MRI image is co-registered to the DWI image (b = 0 image) and the forward transformation parameters mapping the transformation from T_1-weighted-MRI space (M matrix) and its inverse transformation parameters (M^{-1} matrix) are saved. Step 2: The T_1-weighted-MRI image is also segmented into grey matter (GM, accounting for brain size by multiplying with the Jacobian determinants) and spatially normalized to MNI space, and the warping parameters mapping the normalization from native MRI to MNI space (W matrix) and its inverse (W^{-1} matrix) are also saved. Step 3: The W^{-1} and M matrix transformations are

(continued)

DTI data processing

The DWI-SE images for all subjects were pr-processed using the FSL 5.0.9 Diffusion Toolbox (Smith *et al.*, 2004) (FDT) (http://fsl.fmrib.ox.ac.uk/fsl/fslwiki/FDT). For each subject, the DWI images were first corrected for distortions due to Eddy currents and aligned to the b = 0 s/mm^2 image using rigid-body registration for motion correction. Then, diffusion parameters at each voxel in the whole brain were first estimated using latest version of BEDPOST (Behrens *et al.*, 2003). The resulting distributions were then used for connectivity-based classification of the thalamus using the latest version of PROBTRACK (Behrens *et al.*, 2007). The algorithm evaluates connectivity values between the seed (thalamus) and the target masks defined *a priori*. The target masks used in the present study were (i) 'frontal-executive', which included BA9 and BA46; (ii) 'cerebellar-executive' consisting of cerebellar crus I and II; (iii) 'frontal-motor' containing the precentral gyrus; (iv) 'cerebellar-motor': cerebellar lobes IV–VI, as key nodes of the FCC; and (v) hippocampus as a key node for the Papez circuit. The classification was carried out in native DTI space. The output from PROBTRACK was a seed image for each target (five images per subject) in which each voxel held the number of samples from that voxel to the relevant target mask. The value of all voxels outside the seed mask was zero. The number of samples in a thalamic voxel effectively refers to the number of streamlines in that voxel that will reach the target region. It represents a quantitative indication of the likelihood of a path existing between the seed and target region. The higher the number, the higher the likelihood that seed and target region are well connected, thus providing an indication of the global connectivity existing between them.

Extracting number of samples and volumes

Using the five seed images, the thalamus was then individually segmented by classifying each of its voxels as belonging to the target mask with the highest number of samples, reflecting the highest connection probability (Behrens *et al.*, 2003, 2007). Thalamic voxels could be wrongly segmented as reflected by a low number of samples for each target mask in the seed images (Fig. 2). A low number of samples can be recorded in a voxel for two main reasons. First, it can be related to the fact that the voxel is effectively connected to a region that has not been defined as an *a priori* target mask. The number recorded is thus noise in the data and should be ignored. Second, the pathology can result in a disconnection between the thalamus and a specific brain region such that the number of samples decreases drastically. Despite its low value, this voxel should not be ignored in the subsequent calculation of the mean number of samples connected to the target mask. Prior to performing a hard segmentation of the thalamus, the seed images had to be thresholded to eliminate noise while keeping the voxels in which low values could be explained by the inherent pathology. To date, there is no standard methodology regarding thresholding of the number of samples resulting from probabilistic tractography to cater for noise (Morris *et al.*, 2008). Previous studies have intuitively chosen to threshold data at $n = 2$ from 5000 (Fan *et al.*, 2016), $n = 10$ from 5000 (Heiervang *et al.*, 2006); $n = 25$ of 25 000 samples (Johansen-Berg *et al.*, 2007). The use of histograms has allowed for a data-driven way of selecting a threshold value. Histograms are useful as they allow for a visual representation of data distributions, hence facilitating the localization of noise within the data, observed as a high frequency of low numbers on the plot (Fig. 2). For the control group, the noise distribution becomes less as the histograms start to 'plateau'. However, for the patient groups, the 'curve' before the plateau could be important, as these values could be a mixture of noise and a low number of samples due to the inherent pathology (Fig. 2). In the absence of a gold standard as to how to threshold such measurements, we drew a horizontal line where the histograms generally start to curve, measured the corresponding x-values (number of samples) and calculated an average of those measurements. This cut-off number was found to be equal to 35. Nevertheless, this threshold value remains an approximation that would very likely vary due to sample size, or different patient groups.

Post-segmentation, the mean number of samples in each parcellation was calculated for each subject in their native space. To calculate the volumes of these parcellations, the segmented thalami for each subject were warped to their corresponding grey matter volumes in MNI space by applying the forward transformation parameters from the normalization process and the sum of the number of modulated grey matter voxels calculated from there.

The digital thalamic atlas (Krauth *et al.*, 2010), derived from histological data, was used to identify the parcellations that the target regions were connected to. This was conducted in controls first (to visually assess for consistency) and then in each patient.

Statistical analyses

For each thalamic parcellation, one-way analysis of covariance (ANCOVA) was performed to analyse group effect (healthy controls, uncomplicated alcoholics, and Korsakoff's syndrome) for connectivity measures (mean number of samples) and volumes with age, gender and total intercranial volume as covariates. The main effects were corrected for multiple comparisons

Figure 1 Continued
successively applied to the target masks in MNI space to put them into DTI native space. Step 4: The diffusion parameters are estimated using BEDPOST. Step 5: The number of connections from each target mask to the seed mask (thalamus) is estimated using PROBTRACK, which outputs one image for each target mask [Result (**A**), five images per subject on the overall]. Step 6: A hard-segmentation is performed on Result (**A**) to produce one image [Result (**B**)] where each voxel within the thalamus is assigned to the target mask that has the highest number of connections. Hence the nuclei are segmented. Step 7: The segmented nuclei are used to calculate the mean number of connections from Result (**A**). Step 8: The corresponding volumes of the nuclei are calculated by transforming Result (**B**) into MNI space using the M^{-1} and W transformation matrices and multiplying by the grey matter volume. $T_1W = T_1$-weighted.

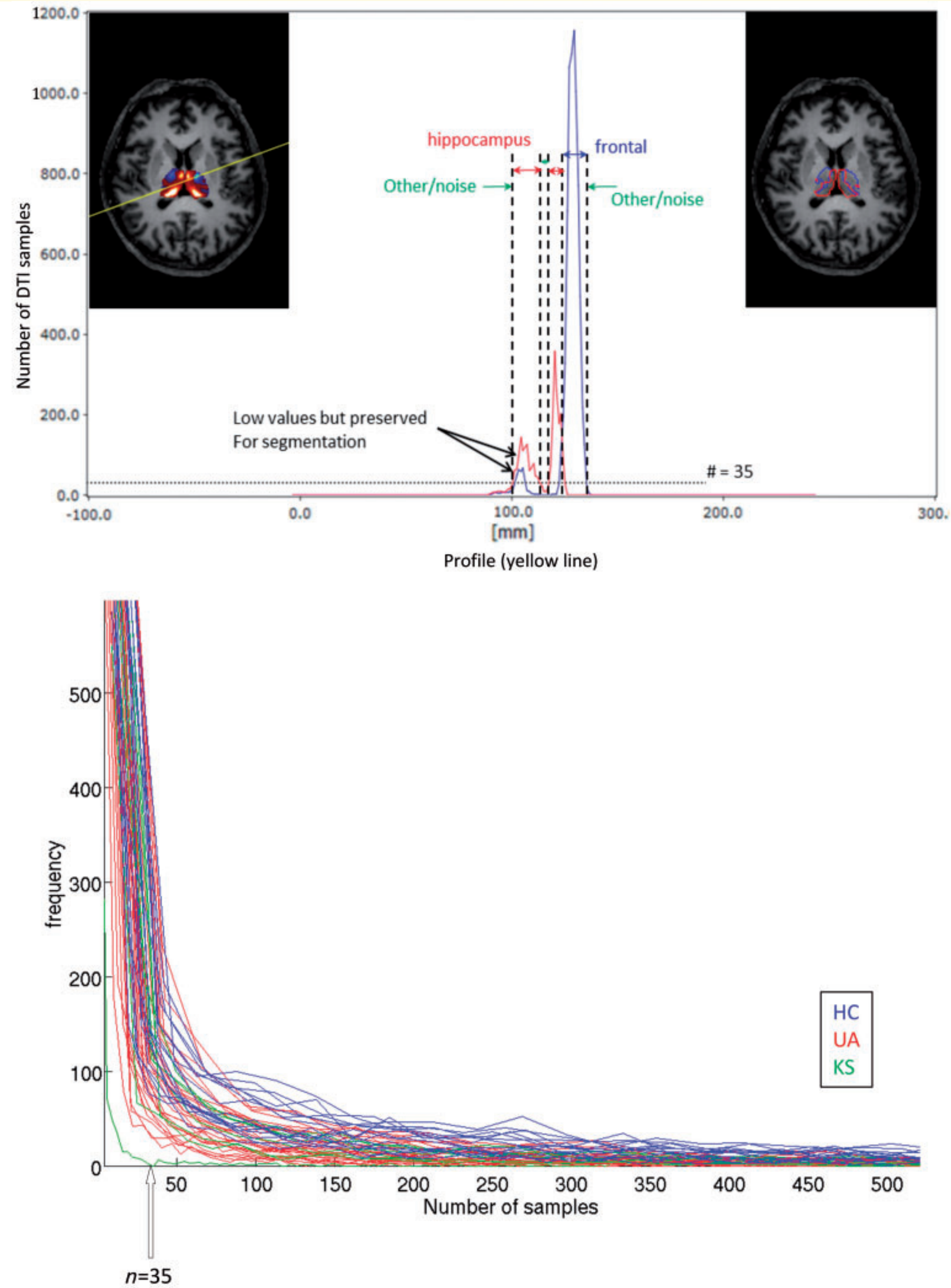

Figure 2 Illustration of the use of histograms to threshold for noise. *Top left* image shows the seed results obtained for targets: hippocampus (red thalamic clusters) and frontal-executive (blue thalamic clusters). The contours of those two clusters are drawn on the *top right* image (red contour for hippocampus as a target and blue contour for the frontal-executive target). A profile has been drawn across the image (yellow line corresponds to *x*-axis on the *top* graph) and the voxel intensities (corresponds to *y*-axis on the *top* graph) in the seed results are plotted on the graph. These voxel intensities correspond to the number of DTI samples for each seed in their respective images. Histograms (*bottom* graph showing number of voxels in seed image containing the corresponding number of DTI samples) show how the cut-off of 35 was selected for thresholding for the frontal executive region. Low values that represent noise are likely to be in the 'vertical' part of the histogram. The range of values lying in the vertical area for all three groups were taken and averaged. This average number for the seeds converged towards n = 35. Beyond n = 35, the voxel values for each seed image for each subject started to plateau such that they can be considered to be part of the connectivity distribution and not noise. This cut-off (n = 35) was consistent for all seed images and was therefore used across the whole dataset. HC = healthy controls; KS = Korsakoff's syndrome; UA = uncomplicated alcoholics.

using a Bonferroni correction accounting for the five thalamic parcellations (new significant P-value < 0.01). The effect sizes for DTI and volumetric measures were also calculated (η^2). *Post hoc* (HSD Tukey, unequal sample sizes) comparisons between healthy control, uncomplicated alcoholic and Korsakoff's syndrome groups were then carried out. Over and above the debates on how multiplicity should be corrected for (Schulz and Grimes, 2005), we also considered the fact that the ANCOVAs already consider the three groups and that volumetric measures are not independent of the connectivity measures. These tests, and the number of comparisons therefore offer a good compromise and maintain the confidence and integrity of our statistical analyses. Correlations between connectivity and volumetric measurements on one hand, and alcohol drinking history on the other hand, with age and gender as covariates, were also carried out.

Data availability

All data and materials used within this study will be made available, upon reasonable request, to research groups wishing to reproduce/confirm our results.

Results

Segmentation results were visually labelled using the thalamic histological atlas (Fig. 3) and revealed that the 'frontal-executive' target had a high number of connections to a major portion of the mediodorsal nuclei and a small part of the ventral anterior nuclei (Krauth *et al.*, 2010). The 'cerebellar-executive' target had a high number of connections essentially to the ventral anterior nuclei and a small part of the mediodorsal nuclei. The 'frontal-motor' target was mainly connected to the ventral lateral and latero-dorsal part of the thalamus, while the 'cerebellar-motor' was mostly connected to the ventral lateral part of the thalamus and part of the lateral geniculate. The hippocampus had a high number of connections to the anterior nuclei and the ventral midline nuclei (part of the mediodorsal nuclei in atlas), pulvinar and latero-dorsal nuclei. For ease of comprehension, the parcellations connected to their respective targets will henceforth be referred to as 'frontal-executive parcellation', 'cerebellar-executive parcellation', 'frontal-motor parcellation', 'cerebellar-motor parcellation' and 'hippocampus-parcellation', respectively.

The ANCOVAs conducted on the connectivity measures showed significant between-group differences for the hippocampus-parcellation only [$F(2,57) = 12.1$; $P < 0.0001$; $\eta^2 = 0.2964$]. *Post hoc* comparisons revealed graded effects from healthy controls to uncomplicated alcoholics ($P = 0.002$) to Korsakoff's syndrome ($P = 0.0001$) and uncomplicated alcoholics to Korsakoff's syndrome ($P = 0.0169$).

Regarding the volumes of the thalamic parcellations, significant differences were observed for the frontal-executive parcellation [$F(2,56) = 18.7$; $P < 0.0001$; $\eta^2 = 0.40$], and hippocampus parcellation [$F(2,56) = 5.5$; $P = 0.0060$; $\eta^2 = 0.170$]. Subsequent *post hoc* comparisons showed lower volumes in the frontal-executive parcellation in uncomplicated alcoholics ($P < 0.0001$) and Korsakoff's syndrome compared to healthy controls ($P < 0.0001$). The hippocampus parcellation had significantly lower volumes only in the Korsakoff's syndrome group compared to healthy controls ($P = 0.0036$). The total volume of the thalamus also differed significantly [$F(2,56) = 12.6$; $P < 0.0001$; $\eta^2 = 0.310$] between the three groups, with graded effects from healthy controls and uncomplicated alcoholics ($P < 0.0001$), healthy controls and Korsakoff's syndrome ($P < 0.0001$) and uncomplicated alcoholics and Korsakoff's syndrome ($P = 0.0275$), both the uncomplicated alcoholic and Korsakoff's syndrome groups being significantly different from healthy controls in *post hoc* comparisons ($P < 0.0001$). For all other parcellations, volumetric differences between uncomplicated alcoholic and Korsakoff's syndrome groups were not significant (Fig. 4).

There were no significant correlations between alcohol drinking history and DTI, or volumetric measurements (all P-values > 0.05).

Discussion

Our results show that connections to the nodes of the FCC and Papez circuit are not limited to one nucleus only within the thalamus. The scientific explanation would be that thalamic nuclei are interconnected and the tractography algorithm independently evaluates the number of samples within each parcellation for every voxel. From a methodological point of view, the overlap between one or more nuclei for each parcel could be a resolution consideration. Nevertheless, the scientific explanation is more potent since it has been shown that the effective resolution of the resulting parcellations should be finer than that of the original diffusion images as the tractography algorithm works on diffusion measurements on a global scale rather than at a voxel level (Johansen-Berg *et al.*, 2005).

The present study showed that the motor loop of the FCC is mostly connected to the ventral lateral and lateral-dorsal part of the thalamus, which is consistent with previous studies showing the functional-anatomical involvement of the thalamus within this loop in healthy subjects (Johansen-Berg *et al.*, 2005) and in patients with tremors (Fang *et al.*, 2016). The absence of between-group difference for the 'frontal-motor parcellations' probably implies that this part of the FCC circuitry is relatively preserved in AUD as has been previously reported (Harper, 2009). On the executive front, the connections between the cerebellum and specific thalamic nuclei have not been well documented in the literature. In fact, the perspective of the cerebellum playing a role in cognition, above motor performances, is fairly new (Buckner, 2013), which in-part explains why no studies in humans have specifically pointed to thalamic nuclei that connect to the cerebellar cruses. The present investigation and previous studies (Behrens *et al.*, 2003; Johansen-Berg *et al.*, 2005) suggest that the nuclei

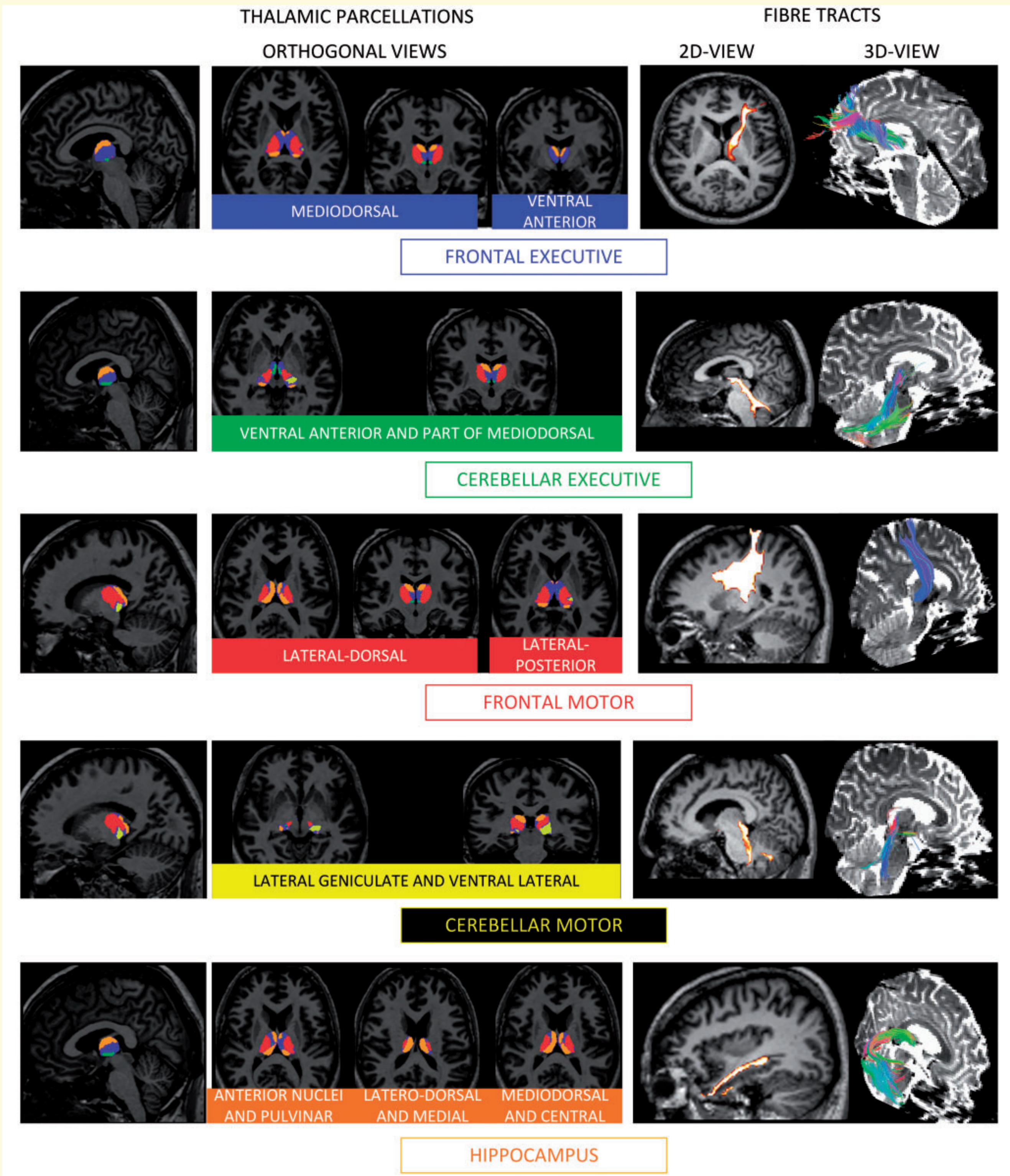

Figure 3 Thalamic parcellations that result from the segmentation using PROBTRACK. The thalamus used as a seed and the targets being the 'frontal-executive' (blue), 'frontal-motor' (red), 'cerebellar-executive' (green), 'cerebellar-motor' (yellow), and hippocampus (orange). *Left* and *middle* columns shows the thalamic parcellations in the orthogonal views. *Right* column shows the fibre tracts that effectively connect the thalamic parcellations to their respective targets, first in 2D view, then in 3D view. These tracts have been produced for graphical representation only. The figure has been rendered from the data of one healthy control in native space. This visual assessment also served as systematic quality control for all 62 participants.

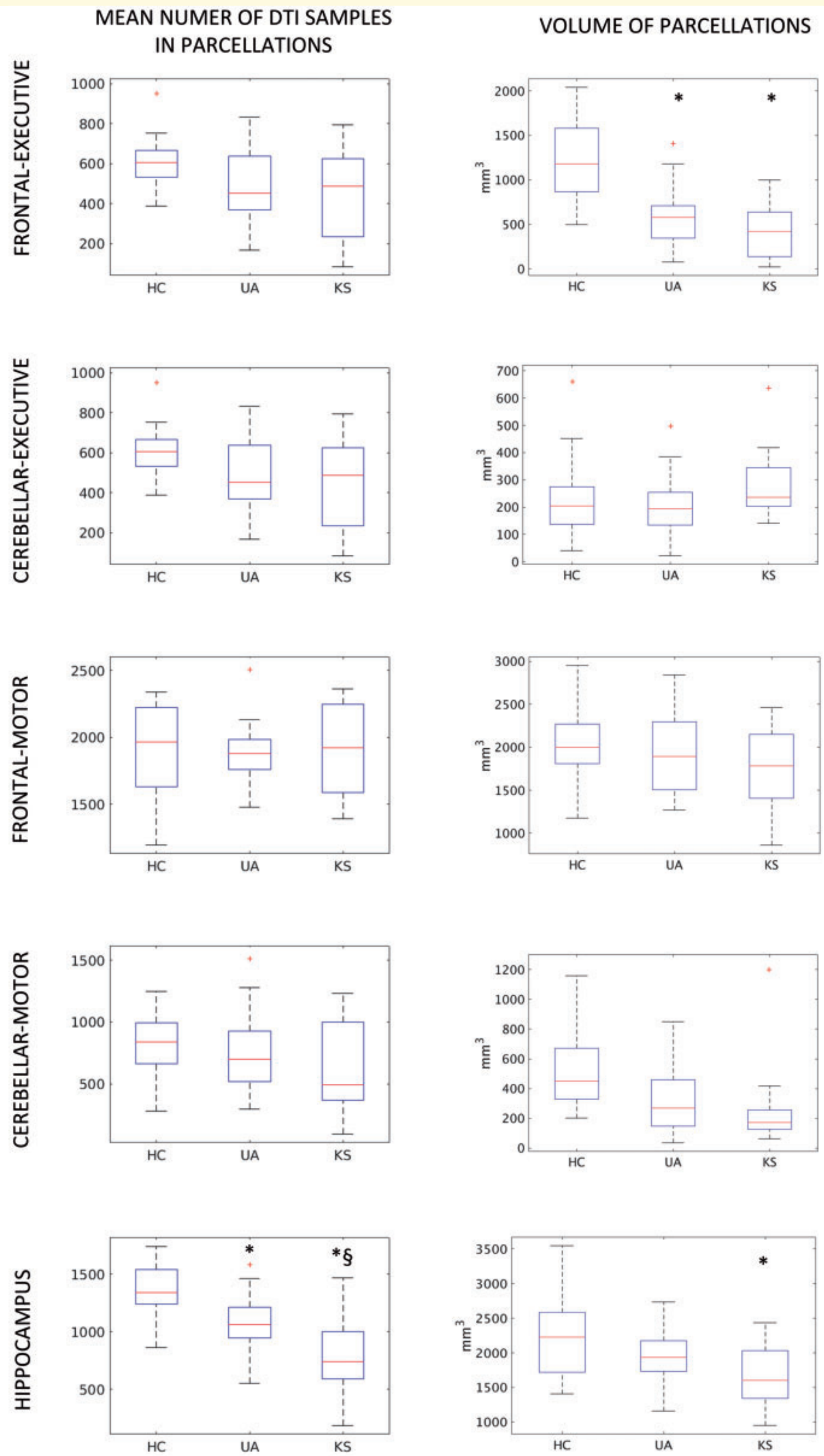

Figure 4 Boxplots showing group comparisons for mean number of DTI samples and volumes for each thalamic parcellation. HC = healthy controls; KS = Korsakoff's syndrome; UA = uncomplicated alcoholics. Plus symbols denote outliers within respective group, included in the statistical comparisons but excluded from boxplots when calculating median, lower and upper percentiles. Asterisk indicates subsequent significant differences between healthy controls and uncomplicated alcoholics. Section sign (§) indicates significant differences between uncomplicated alcoholics and Korsakoff's syndrome (*post hoc*, Tukey, unequal sample sizes) $P < 0.01$ (corrected for multiple comparisons for main effects and at *post hoc* level, Tukey HSD for unequal sample sizes).

connected to the cerebellar-executive regions (ventral anterior and mediodorsal nuclei) are also connected to the frontal part of the executive loop.

That the hippocampus has connections to several thalamic nuclei fits well with the literature on hippocampo-thalamo connectivity. While connections between the anterior nuclei and hippocampus via the fornix is well established, non-fornical projections via the entorhinal cortex to the medial nuclei, pulvinar and part of the lateral-dorsal nuclei have also been observed using tracer techniques in macaques (Saunders *et al.*, 2005). In healthy humans, probabilistic tractography between the medial temporal lobe and the thalamus has confirmed these non-fornical fibre projections (Johansen-Berg *et al.*, 2005). Several animal and human studies (Aggleton and Brown, 1999; Carlesimo *et al.*, 2011, 2014; Mitchell and Chakraborty, 2013), some involving resting state functional MRI (Kafkas and Montaldi, 2014), have highlighted the implication of the mediodorsal nuclei in memory functioning through this non-fornical route. In fact, the implication of which specific nuclei, anterior or mediodorsal, whose lesions contribute directly towards amnesia, has so far been elusive (Mair *et al.*, 2015).

To understand why part of the mediodorsal nuclei, known to be rather involved in higher order cognitive functions than in episodic memory, could contribute to amnesia, calculations were made *a posteriori* using a histological atlas (Krauth *et al.*, 2010). These showed that 83.9% of the anterior nuclei were involved in the hippocampus parcellations (13.9% of the mediodorsal nuclei, 29.2% of pulvinar, and 14.1% of lateral-dorsal). The atlas is known to have limitations regarding accurate quantitation (Pergola, 2016) and does not contain the smaller nuclei, such as the reuniens and rhomboid nuclei, both suspected to be involved in diencephalic amnesia (Barnett *et al.*, 2018). A further detailed visual inspection of the atlas has allowed us to observe that these nuclei are potentially included in the mediodorsal nuclei indices of the atlas, hence offering an alternative explanation to the observed direct connections between the so-called mediodorsal nuclei and the hippocampus and its subsequent implication in memory. Taken together, it can be assumed that it is the anterior nuclei that are mainly and directly connected to the hippocampus. Similar calculations were carried out for the frontal-executive parcellations and it was found that 70.1% of the mediodorsal nuclei were involved in that parcellation. Hence, it can be assumed that the mediodorsal nuclei are mainly connected to the frontal-executive target.

These neuroanatomical findings are crucial to the better understanding of the pathophysiology of AUD as they allow the specification of the nature of the structural damage occurring within thalamic nuclei (Mair *et al.*, 1979; Mayes *et al.*, 1988; Harding *et al.*, 2000). The novelty of the present study is to involve uncomplicated alcoholics and Korsakoff's syndrome patients having brain abnormalities along a continuum that is known to slowly evolve from mild to moderate to severe so that we can concretely formulate a general model of specific thalamic structural alterations happening in the pathology. In AUD, two distinct pathophysiological mechanisms may thus affect the Papez circuit and FCC. In the Papez circuit, disconnection between the hippocampus and its related thalamic parcellation, involving mainly the anterior nuclei, may be leading the alterations. In the FCC, shrinkage of the 'frontal-executive' parcellation, involving mainly the mediodorsal nuclei, seems to be the most prominent. These results are in agreement with previously reported findings in animal, histological and neuroimaging studies that both the anterior and mediodorsal thalamus are severely damaged in Korsakoff's syndrome (Mair *et al.*, 1979; Mayes *et al.*, 1988; Harding *et al.*, 2000; Savage *et al.*, 2012). While the extent of damage to the mediodorsal nuclei is similar in uncomplicated alcoholics and Korsakoff's syndrome, shrinkage of the anterior nuclei seems specific to Korsakoff's syndrome. Having showed that the mechanism that leads the pathophysiology of alterations in the anterior nuclei of the thalamus in AUD is a disconnection, it can be hypothesized that this graded disconnection among AUD groups potentially cascades into atrophy of the anterior thalamus, leading to Korsakoff's syndrome. This would corroborate with case studies in Korsakoff's syndrome that have found disruption of the mammillothalamic tract and lesions within the anterior nuclei and mammillary bodies (Mair *et al.*, 1979; Mayes *et al.*, 1988). A quantitative histological study has also echoed the same findings (Harding *et al.*, 2000), pinpointing the anterior nuclei as being a critical site of damage in patients with Korsakoff's syndrome. Nevertheless, a couple of studies have found the mediodorsal nuclei to be significantly atrophied in Korsakoff's syndrome patients compared to control subjects (Victor *et al.*, 1971), and Korsakoff's syndrome patients compared to both uncomplicated alcoholics and control subjects (Pitel *et al.*, 2012). Over and above the criticism regarding the neuropsychological criteria that were used to fit the aetiology of patients with Korsakoff's syndrome in the study by Victor *et al.* (1971), another potential explanation is that what is identified as being part of the mediodorsal nuclei is in fact a thalamic region that effectively houses the reuniens and rhomboid nuclei involved in memory functions (Barnett *et al.*, 2018). This is also reflected in a neuroimaging study (Pitel *et al.*, 2012) in which, from the results portrayed, atrophy of the thalamus is evident on both the anterior as well as part of the mediodorsal front.

It was surprising to find no significant between-group difference for the 'cerebellar-executive parcellations', which is known to be altered in AUD. The reason could be methodological, as the brainstem, midbrain and cerebellum contain dense crossing fibres that make tracking of pathways difficult. Yet, this did not seem to be the case for the 'cerebellar-motor' target in which the fibre tracts go through these same regions. Another reason could be that the leading mechanism is a demyelination, as reflected through decrease in fractional anisotropy values in the inferior and superior cerebellar peduncles, but is not necessarily accompanied by neuronal death, such that the number of connections does not necessarily decrease. The absence of between-group difference for the 'frontal-motor parcellations' probably implies that this part of the FCC circuitry is relatively preserved in AUD, as has been previously reported.

For the cerebellar-motor parcellation, the presence of an outlier could be a reason why no significant comparisons were observed [$F(2,55) = 3.8782$; $P = 0.0266$ if the outlier is not considered in the statistics]. However, interpretation of results from this parcellation was not deemed comparable to the hippocampus parcellation since no significant results were obtained on the connectivity side. Atrophy of the cerebellar-motor parcellation could therefore be a consequence within the main pathophysiological mechanism of Korsakoff's syndrome.

Methodological and statistical considerations

Cortical atrophy has not been explicitly accounted for. However, it has been indirectly considered as tractography is performed in native space. The seed and target masks have been obtained from MNI space, segmented and normalized into native space and should technically not contain atrophied voxels. However, it is difficult to say whether cortical atrophy needs to be corrected for or not, as structural disconnection could induce atrophy and vice versa. While the relationships between thalamic atrophy and disconnections are complex to interpret at the current stage, what is interesting is that we observe clearly defined mechanisms across two groups of patients that lie along a continuum, such that we can suppose which mechanisms are more prominent in their respective brain circuits, as detailed above.

Conclusion

Overall, the results of this study show, *in vivo* and across a continuum of AUD pathology, that the chronic and excessive consumption of alcohol is associated with structural damage to both the mediodorsal and anterior nuclei. However, despite a relatively small but robust sample size, atrophy of the anterior nuclei has shown a tendency to be specific to patients with Korsakoff's syndrome and offers the prospect of being a neuroimaging marker that could define not only the pathophysiology of Korsakoff's syndrome but also that of other neurological disorders directly linked to thalamic amnesia. Further studies should be geared towards confirming this line of thought.

Funding

This study was funded by Fondation pour la Recherche Medicale (FRM, ING20140129160), ANR-Retour post-doctorant 2010, Conseil Regional Basse Normandie, and MILDECA.

Competing interests

All authors declare no conflict of interest in any form or kind in relation to this study and its publication.

References

Aggleton JP. Multiple anatomical systems embedded within the primate medial temporal lobe: Implications for hippocampal function. Neurosci Biobehav Rev 2012; 36: 1579–6.

Aggleton JP, Brown MW. Episodic memory, amnesia, and the hippocampal-anterior thalamic axis. Behav Brain Sci 1999; 22: 425–44; discussion 444–89.

Barnett SC, Perry BAL, Dalrymple-Alford JC, Parr-Brownlie LC. Optogenetic stimulation: Understanding memory and treating deficits. Hippocampus 2018; 28: 457–70.

Behrens TEJ, Berg HJ, Jbabdi S, Rushworth MFS, Woolrich MW. Probabilistic diffusion tractography with multiple fibre orientations: What can we gain? Neuroimage 2007; 34: 144–55.

Behrens TEJ, Johansen-Berg H, Woolrich MW, Smith SM, Wheeler-Kingshott CAM, Boulby PA, et al. Non-invasive mapping of connections between human thalamus and cortex using diffusion imaging. Nat Neurosci 2003; 6: 750–7.

Behrens TEJ, Woolrich MW, Jenkinson M, Johansen-Berg H, Nunes RG, Clare S, et al. Characterization and propagation of uncertainty in diffusion-weighted MR imaging. Magn Reson Med 2003; 50: 1077–88.

Buckner RL. The cerebellum and cognitive function: 25 years of insight from anatomy and neuroimaging. Neuron 2013; 80: 807–15.

Carlesimo GA, Lombardi MG, Caltagirone C. Vascular thalamic amnesia: a reappraisal. Neuropsychologia 2011; 49: 777–89.

Carlesimo GA, Lombardi MG, Caltagirone C, Barban F. Recollection and familiarity in the human thalamus. Neurosci Biobehav Rev 2014; 54: 18–28.

Chanraud S, Pitel A-L, Rohlfing T, Pfefferbaum A, Sullivan EV. Dual tasking and working memory in alcoholism: relation to frontocerebellar circuitry. Neuropsychopharmacology 2010; 35: 1868–78.

Cushman PJ, Forbes R, Lerner W, Stewart M. Alcohol withdrawal syndromes: clinical management with lofexidine. Alcohol Clin Exp Res. 1985; 9: 103–8.

Fan L, Li H, Zhuo J, Zhang Y, Wang J, Chen L, et al. The human brainnetome atlas: a new brain atlas based on connectional architecture. Cereb Cortex 2016; 26: 3508–26.

Fang W, Chen H, Wang H, Zhang H, Puneet M, Liu M, et al. Essential tremor is associated with disruption of functional connectivity in the ventral intermediate Nucleus-Motor Cortex-Cerebellum circuit. Hum. Brain Mapp 2016; 37: 165–78.

Gache P, Michaud P, Landry U, Accietto C, Arfaoui S, Wenger O, et al. The Alcohol Use Disorders Identification Test (AUDIT) as a screening tool for excessive drinking in primary care: reliability and validity of a French version. Alcohol Clin Exp Res 2005; 29: 2001–7.

Harding A, Halliday G, Caine D, Kril J. Degeneration of anterior thalamic nuclei differentiates alcoholics with amnesia. Brain 2000; 123 (Pt 1): 141–54.

Harper C. The neuropathology of alcohol-related brain damage. Alcohol Alcohol 2009; 44: 136–40.

Heiervang E, Behrens TEJ, Mackay CE, Robson MD, Johansen-Berg H. Between session reproducibility and between subject variability of diffusion MR and tractography measures. Neuroimage 2006; 33: 867–877.

Johansen-Berg H, Behrens TEJ, Sillery E, Ciccarelli O, Thompson AJ, Smith SM, et al. Functional-anatomical validation and individual variation of diffusion tractography-based segmentation of the human thalamus. Cereb Cortex 2005; 15: 31–9.

Johansen-Berg H, Della-Maggiore V, Behrens TEJ, Smith SM, Paus T. Integrity of white matter in the corpus callosum correlates with bimanual co-ordination skills. Neuroimage 2007; 36 (Suppl 2): T16–21.

Kafkas A, Montaldi D. Two separate, but interacting, neural systems for familiarity and novelty detection: A dual-route mechanism. Hippocampus 2014; 24: 516–27.

Kelly RM, Strick PL. Cerebellar loops with motor cortex and prefrontal cortex of a nonhuman primate. J Neurosci 2003; 23: 8432–44.

Kopelman MD. What does a comparison of the alcoholic Korsakoff syndrome and thalamic infarction tell us about thalamic amnesia? Neurosci Biobehav Rev 2015; 54: 46–56.

Kopelman MD, Thomson AD, Guerrini I, Marshall EJ. The Korsakoff syndrome: clinical aspects, psychology and treatment. Alcohol Alcohol 2009; 44: 148–54.

Krauth A, Blanc R, Poveda A, Jeanmonod D, Morel A, Székely G. A mean three-dimensional atlas of the human thalamus: generation from multiple histological data. Neuroimage 2010; 49: 2053–62.

Mair RG, Miller RLA, Wormwood BA, Francoeur MJ, Onos KD, Gibson BM. The neurobiology of thalamic amnesia: contributions of medial thalamus and prefrontal cortex to delayed conditional discrimination. Neurosci Biobehav Rev 2015; 54: 161–74.

Mair WGP, Warrington EK, Weiskrantz L. Memory disorder in Korsakoff's psychosis: a neuropathological and neuropsychological investigation of two cases. Brain 1979; 102: 749–783.

Mayes AR, Meudell PR, Mann D, Pickering A. Location of Lesions in Korsakoff's syndrome: neuropsychological and neuropathological data on two patients. Cortex 1988; 24: 367–388.

Mitchell AS, Chakraborty S. What does the mediodorsal thalamus do? Front Syst Neurosci 2013; 7: 37.

Mori S, van Zijl PCM, Oishi K, Faria A V. MRI atlas of human white matter. 2nd edn. London: Elsevier Science; 2010.

Morris DM, Embleton KV, Parker GJM. Probabilistic fibre tracking: differentiation of connections from chance events. Neuroimage 2008; 42: 1329–39.

Papez J. A proposed mechanism of emotion. Arch Neurol Psychiatry 1937; 28: 725–43.

Pergola G. Thalamic amnesia after infarct: the role of the mammillothalamic tract and mediodorsal nucleus. Neurology 2016; 86: 1928.

Pfefferbaum A, Rosenbloom M, Crusan K, Jernigan TL. Brain CT. Changes in alcoholics: effects of age and alcohol consumption. Alcohol Clin Exp Res 1988; 12: 81–7.

Pitel AL, Beaunieux H, Witkowski T, Vabret F, de la Sayette V, Viader F, et al. Episodic and working memory deficits in alcoholic Korsakoff patients: the continuity theory revisited. Alcohol Clin Exp Res 2008; 32: 1229–41.

Pitel AL, Chételat G, Le Berre a P, Desgranges B, Eustache F, Beaunieux H. Macrostructural abnormalities in Korsakoff syndrome compared with uncomplicated alcoholism. Neurology 2012; 78: 1330–3.

Pitel AL, Segobin SH, Ritz L, Eustache F, Beaunieux H. Thalamic abnormalities are a cardinal feature of alcohol-related brain dysfunction. Neurosci Biobehav Rev 2014; 54: 38–45.

Saunders RC, Mishkin M, Aggleton JP. Projections from the entorhinal cortex, perirhinal cortex, presubiculum, and parasubiculum to the medial thalamus in macaque monkeys: identifying different pathways using disconnection techniques. Exp Brain Res 2005; 167: 1–16.

Savage LM, Hall JM, Resende LS. Translational rodent models of Korsakoff syndrome reveal the critical neuroanatomical substrates of memory dysfunction and recovery. Neuropsychol Rev 2012; 22: 195–209.

Schulz KF, Grimes DA. Multiplicity in randomised trials I: endpoints and treatments. Lancet 2005; 365: 1591–95.

Segobin S, Ritz L, Lannuzel C, Boudehent C, Vabret F, Eustache F, et al. Integrity of white matter microstructure in alcoholics with and without Korsakoff's syndrome. Hum Brain Mapp 2015; 36: 2795–808.

Sherman SM, Guillery RW. Chapter {III} - the afferent axons to the thalamus. In: Guillery SMSW, editor. Exploring the Thalamus. San Diego: Academic Press; 2001. p. 59–107.

Smith SM, Jenkinson M, Woolrich MW, Beckmann CF, Behrens TEJ, Johansen-Berg H, et al. Advances in functional and structural MR image analysis and implementation as FSL. Neuroimage 2004; 23 (Suppl): S208–19.

Spielberger CD, Gorsuch RL, Lushene R, Vagg PR JG. Manual for the state-trait anxiety inventory (form Y). Palo Alto: Consulting Psychologists Press; 1983.

Sullivan E V, Pfefferbaum A. Neuroimaging of the Wernicke-Korsakoff syndrome. Alcohol Alcohol 2008; 44: 155–65.

Victor M, Adams RD, Collins GH. The Wernicke-Korsakoff syndrome. Philadelphia: F.A. Davis Co.; 1971.